CrystEngComm

Accepted Manuscript

ROYAL SOCIETY OF CHEMISTRY

www.rsc.org/crystengcomm

Facile fabrication of graphene-topological insulator Bi_2Se_3 hybrid Dirac materials via chemical vapor deposition in Se-rich condition

C Zhang[a] , M Liu[a] , B Y Man[a, *], S Z Jiang[a,c] , C Yang[a], C S Chen[a] , D J Feng[b] , D Bi[a] , F Y Liu[a] , H W Qiu[a] and J X Zhang[a]

[a] *College of Physics and Electronics, Shandong Normal University, Jinan, 250014, People's Republic of China*

[b] *School of Information Science and Engineering, Shandong University，Jinan, 250100, People's Republic of China*

[c] *State Key Lab of Crystal Materials Shandong University, Jinan, 250100, People's Republic of China*

Abstract

Direct deposition of uniform and high-quality Bi_2Se_3 thin film on graphene film (layer controlled) is offered using a catalyst-free vapor deposition system in Se-rich environment. The Se-rich environment is utilized to fill the Se vacancies and beneficial to the uniform chemical composition of the product. The layers of the graphene can be controlled easily and precisely by the transfer times. Besides the graphene film, the morphology of the product is sensitive to the growth parameters (temperature of the substrate, growth time and gas flow). By controlling the growth parameters, we can also grow crystal Bi_2Se_3 plate on the graphene/SiO_2/Si substrate. Raman spectroscopy, scanning electron microscopy, transmission electron microscopy

[*] *To whom correspondence should be addressed: byman@sdnu.edu.cn (B Y Man)*

and X-ray diffraction confirm the presence of uniform and high-quality Bi_2Se_3.

Introduction

Graphene and topological insulator (such as Bi_2Se_3 and Bi_2Te_3), as typical Dirac materials, have been attracting extensively scientific interests from both experimental and theoretical communities in the recent years as a result of their distinctive band structures and physical properties. As a single-atom-thick sheet of hexagonally arrayed sp^2-bonded carbon atoms, graphene has been reported by numerous articles on the growth method,[1-5] properties (such as optical, electrical and physical properties),[6-8] and technological applications in the various areas.[9-12] Since its discovery, Bi_2Se_3, a reference topological insulator material (a large nontrivial bulk gap ~ 0.3 eV), has also been paid special attentions.[13-16] Motivated by their advantages, attempts to combine these Dirac materials have been made to obtain graphene-Bi_2Se_3 hybrid for future electronic and spintronic applications. Dang et al present a simple vapor-phase deposition of ultrathin Bi_2Se_3 nanoplates on a few-layer pristine graphene substrate by van der Waals epitaxy.[13] However, the layer of the graphene by micromechanical cleavage in the prepared heterostructures of Bi_2Se_3, can not be controlled easily and precisely. It has been demonstrated that chemical vapor deposition (CVD) is an effective method for synthesizing these Dirac materials. What's more, the graphene layers fabricated via CVD can be controlled easily and precisely. Remarkably, graphene serving as a superb substrate for growing high-quality Bi_2Se_3 films has been demonstrated.[17] Here, we offer a catalyst-free CVD method for the fabrication of the graphene-Bi_2Se_3 hybrid with controlled graphene

layers on the SiO_2/Si substrate in Se-rich environment. We note that high-quality single-crystal Bi_2Se_3 thin film and plate can be successfully formed on the graphene film in our case by controlling the growth parameter.

Experimental Method

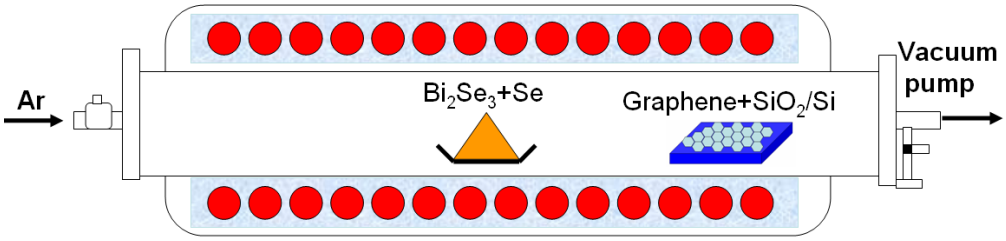

Fig 1. Schematic of the hot-wall CVD system used in this study.

As shown in the Fig. 1, Bi_2Se_3 thin film was deposited on the graphene/SiO_2/Si substrate (G/SiO_2/Si) using a catalyst-free CVD method in the horizontal quartz tube (~2.5 inch in diameter). Before this CVD treatment for the formation of Bi_2Se_3 thin film, we used a similar CVD method to prepare monolayer graphene film on the Cu foil and then transferred it to the oxidized silicon wafer (300 nm SiO_2/Si) substrate with assist of the $FeCl_3$. The layers of the transferred graphene can be controlled by the transfer times. Bi_2Se_3 powder mixed with Se powder (weight ratio ~6:1), as the precursors for evaporation, was located in the constant-temperature zone and the G/SiO_2/Si substrate was placed on a quartz boat in the downstream zone (~15 cm away from constant-temperature zone). Next the horizontal quartz tube was pumped to 1.0×10^{-6} Torr and supplied with ultrapure Ar for 15 min to remove oxygen residue. Then, the tube was heated to the growth temperature (~500 ℃) in the gas flow of the Ar (~56 sccm). Upon reaching the growth temperature, the growth conditions

were maintained for 15 min. Finally, the furnace was naturally cooled down to the ambient temperature in the gas flow of the Ar (~56 sccm).

Following the growth, the morphology of the graphene-Bi_2Se_3 hybrid was characterized by scanning electron microscope (SEM, Zeiss Gemini Ultra-55) with energy-dispersive X-ray spectroscopy (EDX) for chemical analysis. In order to characterize the structural properties of the Bi_2Se_3 thin film, we carried out the Raman spectra on the sample with a Horiba HR Evolution 800 Raman microscopy system (laser wavelength 532 nm). The single-crystalline structure of the Bi_2Se_3 thin film was analyzed with a transmission electron microscopy system (TEM, JEM-2100F), selected area electron diffraction (SAED) and X-ray diffraction (XRD, Bruker D8).

Results and discussion

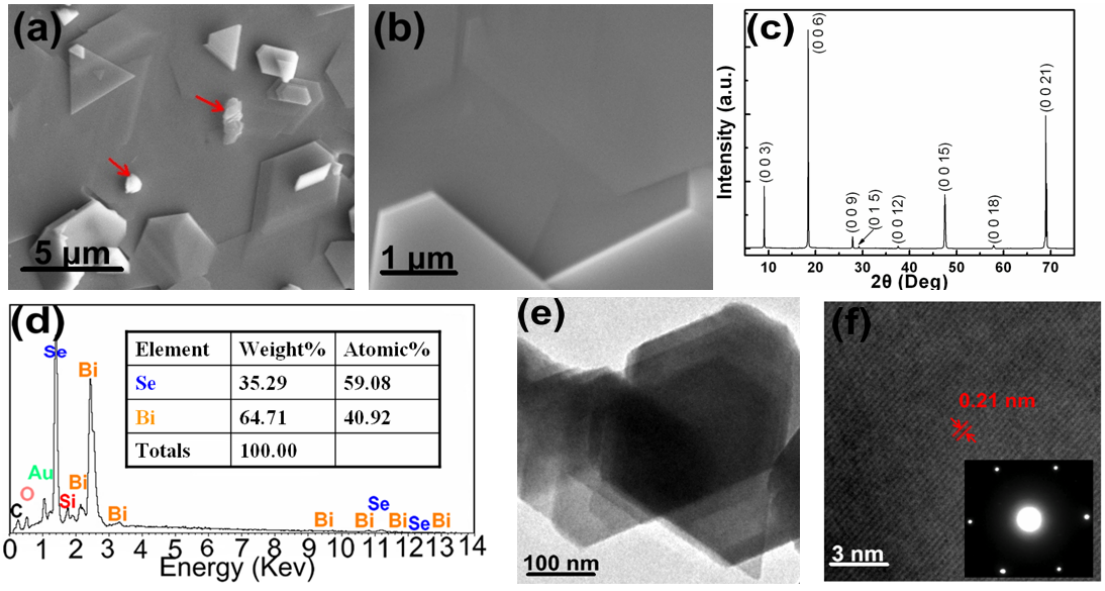

Fig 2. (a) and (b) are the SEM images of the Bi_2Se_3 thin film deposited on the $G/SiO_2/Si$ substrate under different magnification. (c) 2θ-ω X-ray diffraction pattern of the prepared sample. (d) EDX data of the $G/SiO_2/Si$ substrate after the CVD treatment. Insert: quantitative atomic analysis of the Bi and Se element. (e) TEM

image of the Bi_2Se_3 thin film. (f) High-resolution TEM image of the same sample. Insert: the SAED pattern.

Fig. 2(a) exhibits the SEM image of the G/SiO_2/Si substrate after the growth of the Bi_2Se_3 thin film. Coalesced plates of triangular and hexagonal shape, which are aligned in the same orientation on the graphene layer, are well seen. Very few irregular-shape islands marked with the red arrows in Fig. 2(a) are also appreciated, which can be attributed to the random and unsystematic deposition of the vapor-phase Bi_2Se_3 precursor in the naturally cooling process. It is noted that the naturally cooling process can effectively reduce the irregular-shaped islands, however, it is unavoidable that very few vapor-phase Bi_2Se_3 precursor deposits on the surface of the Bi_2Se_3 thin film and forms the irregular-shaped islands. The SEM image displayed in Fig. 2(b) shows that the edges of the hexagonal shape plates array parallelly, which indicates that the Bi_2Se_3 plates are mainly along the direction of 0°, 60°, and 120°.[13] Some Bi_2Se_3 plates deviated from these major directions are also detected as shown in Fig. 2(a). This phenomenon probably arises from the weak van der Waals interaction, defects of the graphene substrate or lattice mismatch.[13] It is possible to investigate the crystal structure of Bi_2Se_3 thin film by XRD measurements. As the XRD analysis provided in Fig 2(c), only the (003) family diffraction peaks are observed, which confirms the rhombohedral structure of the prepared Bi_2Se_3 thin film (a=0.41396nm, c=2.8636nm, PDF Card No. 33-0214) and suggests the high film quality. Based on the details of the XRD peaks, we can identify that the Bi_2Se_3 thin film is c-axis oriented Bi_2Se_3 phase and the quintuple layer spacing of it is ~9.6 Å. EDX results (Fig. 2(d))

show direct and striking evidence that the Bi_2Se_3 thin film deposited on the G/SiO_2/Si substrate possesses uniform chemical composition (atomic ratio Bi:Se=2:3), indicating the film free of impurities within the detectable resolution limit of the EDX. The Bi_2Se_3 thin film is prepared in Se-rich condition in our case, which can effectively fill the Se vacancies and results in the uniform chemical composition. In fact, we also attempt to fabricate high-quality and single-crystal Bi_2Se_3 thin film just with pure Bi_2Se_3 powder as the precursors for evaporation. Nevertheless, we can not obtain Bi_2Se_3 thin film with uniform chemical composition, on the contrary some Se vacancies are detected in the sample. To further verify the crystalline structure of the Bi_2Se_3 thin film, we conducted TEM characterization on the as-prepared sample. The Bi_2Se_3 plates were mechanically transferred from the G/SiO_2/Si substrate to a lacey carbon support film on the copper grid with the assist of a drop of dilute ethyl alcohol solution (2% V/V). Typical low-magnification TEM image of the sample is shown in Fig. 2(e). Stacked triangular and hexagonal plates are clearly visible and the edges of the plates array parallelly. The lateral dimension of the plates is several hundreds nanometers. The hexagonal lattice fringes, with a lattice spacing of 0.21 nm, are well revealed in the HR-TEM image (Fig. 2(f)), which is consistent with the inter spacing of the (11-20) planes. The SAED inserted in Fig. 2(f) exhibits a distinct sixfold symmetric symmetry spot pattern, which confirms the single crystalline nature of the Bi_2Se_3 thin film and is well agreement with the XRD analysis.

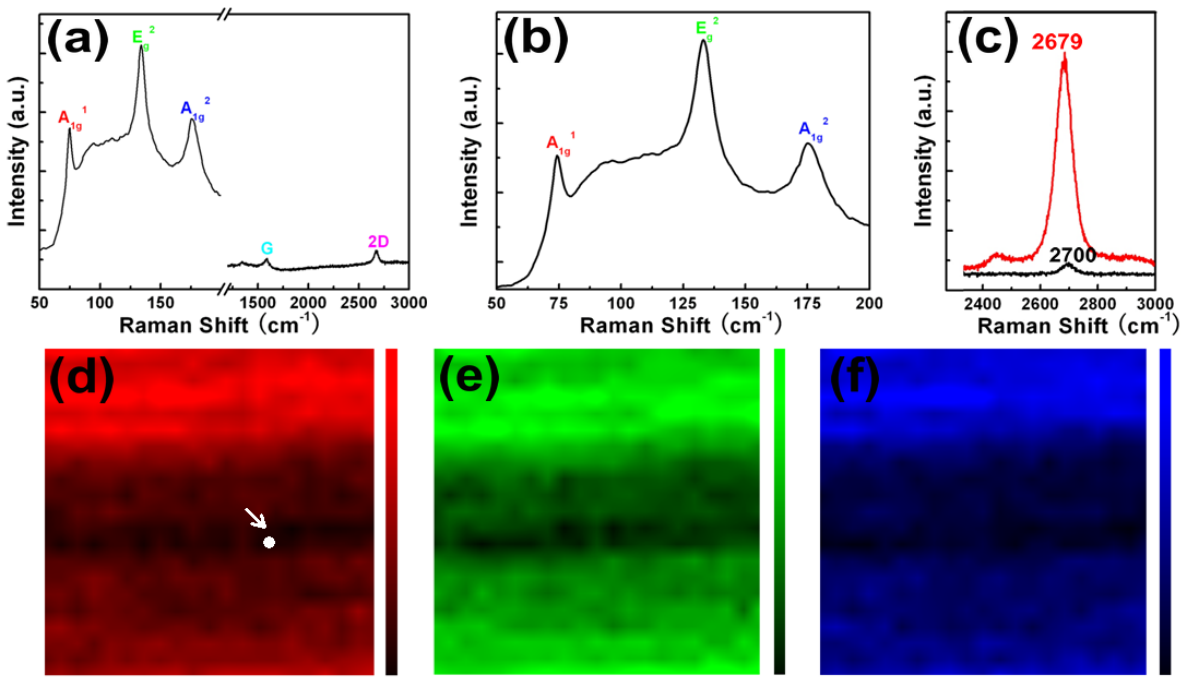

Fig 3. (a) The Raman spectrum of the Bi_2Se_3 thin film deposited on the G/SiO_2/Si substrate. (b) Raman spectrum from the point marked in (d) by the white arrow and dot. (c) Close-up view of 2D bands of the same G/SiO_2/Si substrate before (red) and after (black) the deposition of the Bi_2Se_3 thin film, respectively. (d)-(f) are respectively the scanning Raman A_{1g}^1, E_g^2 and A_{1g}^2 band mappings of a continuous Bi_2Se_3 thin film directly deposited on the G/SiO_2/Si substrate.

In order to give a more definite identification of the Bi_2Se_3 thin film, Raman spectra were carried out on the sample at room temperature using 532 nm excitation laser, with a low power levels (P<0.4 mW) to avoid sample damage. Typical Raman spectrum of the Bi_2Se_3 thin film on the G/SiO_2/Si substrate is shown in Fig. 3(a). Three characteristic bands of the rhombohedral Bi_2Se_3 : ~72, ~131 and ~174 cm^{-1} respectively corresponded to the A_{1g}^1, E_g^2 and A_{1g}^2 vibrational modes,[18] are detected in the low frequency region. In the high frequency region, the spectrum also reveals obvious G and 2D bands at ~1585 and ~2700 cm^{-1}, which are typical signatures of graphene

film. These features imply the fact that the Bi_2Se_3 thin film are successfully fabricated on the surface of G/SiO_2/Si substrate and the graphene film still possesses perfect structural properties after the deposition of the Bi_2Se_3 thin film. Fig. 3(c) presents a clear view of the 2D bands of the same G/SiO_2/Si substrate before (red) and after (black) the deposition of the Bi_2Se_3 thin film, respectively. After the deposition of the Bi_2Se_3 thin film, the 2D band of the monolayer graphene film becomes broader and up shift, which probably can be attributed to the interaction of Bi_2Se_3 thin film and graphene.[13] Fig. 3(d)-3(f) show the 10×10 μm^2 Raman A_{1g}^1, E_g^2 and A_{1g}^2 band mappings of a continuous Bi_2Se_3 thin film directly deposited on the G/SiO_2/Si substrate. As can be seen from Fig. 3(d), 3(e) and 3(f), relatively smooth A_{1g}^1, E_g^2 and A_{1g}^2 band mappings with only a little black region are revealed, which indicates that the prepared Bi_2Se_3 thin film features a micro-scale inhomogeneity and a uniform structure. It is noteworthy that the Raman A_{1g}^1, E_g^2 band mappings correspond well with the A_{1g}^2 band mapping. The Raman spectrum in Fig. 3(c), taken from the region marked by the white dot and arrow in Fig. 3(d), presents typical characteristics of Bi_2Se_3 film: obvious A_{1g}^1, E_g^2 and A_{1g}^2 bands at ~72, ~131 and ~174 cm^{-1}. These Raman results implicate that the uniform Bi_2Se_3 thin film can be directly fabricated on the G/SiO_2/Si substrate.

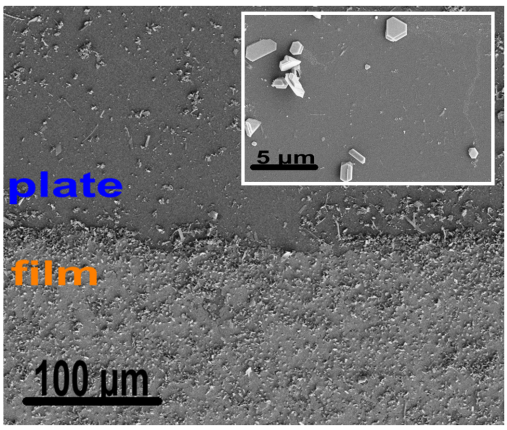

Fig. 4 SEM image of the Bi_2Se_3 grown on the SiO_2/Si substrate (the top region) and on the G/SiO_2/Si substrate (the below region) performed on the edge region of the same sample prepared above. Insert: SEM image of the top region with a large magnification.

SEM image (Fig. 4) gives us convincible evidence that the graphene film plays a crucial role in the formation of the uniform Bi_2Se_3 thin film. Bi_2Se_3 thin film was not detected on the top region in Fig. 4 without graphene film acting as medium layer, on the contrary, Bi_2Se_3 plate was obtained (insert in Fig. 4). As we all known, the quintuple layer of the Bi_2Se_3 in the sequence of Se-Bi-Se-Bi-Se is covalently bonded together via van der Waals interactions, which is similar to the layered structure of graphene. Although there exists a lattice mismatch of ~2.9% between Bi_2Se_3 crystal structure and graphene, the van der Waals interactions of the Bi_2Se_3 crystal structure and graphene, can efficiently suppress the negative effects of the lattice mismatch and make the formation of the Bi_2Se_3 thin film facile and easy. The uniform temperature of the G/SiO_2/Si substrate compared with that of the SiO_2/Si substrate, which can be owe to the existence of the graphene film, may be another crucial factor for the formation of the Bi_2Se_3 thin film. The thermal vibrations are relatively mild in the region,

therefore, vapor-phase Bi_2Se_3 precursor can deposit on the $G/SiO_2/Si$ substrate easily in this case. In fact, we also attempt to deposit Bi_2Se_3 thin film on the $G/SiO_2/Si$ substrate at 600℃ (the other conditions are the same with above). However, only Bi_2Se_3 paltes are obtained (the results not shown here), which verifies the fact that the temperature of the $G/SiO_2/Si$ substrate also plays an important role in the grow process of the Bi_2Se_3 thin film.

To investigate the crucial role of the other growth parameters (the growth time and gas flow) for the direct growth of Bi_2Se_3 thin film on the $G/SiO_2/Si$ substrate, we carried out two contrast experiments. In the contrast experiment Ⅰ, we reduce the growth time from 15min to 10 min and the other growth conditions are the same as those presented above. In the contrast experiment Ⅱ, we change the gas flow of Ar from 56 sccm to 200 sccm, the other growth conditions are the same as those presented above.

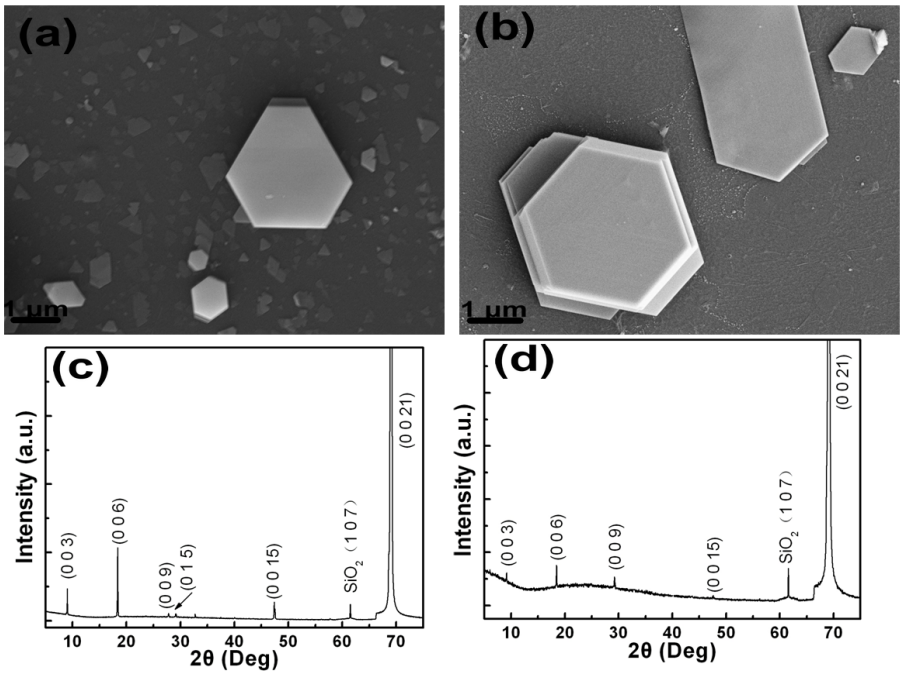

Fig. 5 (a) and (b) are respectively the SEM images of the samples obtained in the

contrast experiments Ⅰ and Ⅱ. (c) and (d) are respectively 2θ-ω X-ray diffraction patterns of the samples obtained in the contrast experiments Ⅰ and Ⅱ.

Fig. 5(a) provides the SEM image of the sample prepared in the contrast experiments Ⅰ. Numerous isolated Bi_2Se_3 plates can be viewed clearly in the shape of triangle and hexagon, and few coalesced plates can also be detected. This phenomenon indicates that by controlling the growth time, we can regulate the morphology (plate or film) of the product in our CVD case. The XRD result (Fig. 5(c)) confirms the crystalline nature of the grown Bi_2Se_3 plates. Fig. 5(b) shows us a clear view of the sample obtained in the contrast experiments Ⅱ. We also fabricate Bi_2Se_3 plates, instead of thin film in this condition. The product also features good crystallinity, just as shown in the Fig. 5(d). However, in the contrast experiments Ⅱ, we have not detected the coalesced Bi_2Se_3 plates and the density of the plates is relative smaller than that obtained in the contrast experiments Ⅰ. These features can be attributed to the large gas flow in the growth process. At large gas flow rate, the vapor-phase Bi_2Se_3 precursor has a short residence time on the G/SiO_2/Si substrate, leading to the lack of the initial activated Bi_2Se_3 nucleus, so only isolated Bi_2Se_3 plates can be formed in the contrast experiments Ⅱ.

Conclusions

In conclusion, we have demonstrated the direct growth and deposition of uniform and high-quality Bi_2Se_3 on the G/SiO_2/Si substrate. The graphene medium layer, temperature of the substrtate, growth time and gas flow is crucial for the facile synthesis of Bi_2Se_3 crystal material. The influencing mechanism of these growth

parameters are discussed in detail. We can successfully obtain Bi_2Se_3 thin film and paltes in our case. This method presents us a promising and economical technique for fabrication of the Bi_2Se_3 thin film and plates and will promote the practical applications of this magical material.

Acknowledgments

The authors are grateful for financial support from the National Natural Science Foundation of China (11274204, 61205174, 61307120 and 61377043), Science and Technology Planning Project of Higher Education of Shandong Province (J11LA14).

References

1 M. Terrones, N. Grobert, J. Olivares, J. P. Zhang, H. Terrones, K. Kordatos, W. K. Hsu, J. P. Hare, P. D. Townsend, K. Prassides, A. K. Cheetham, H. W. Kroto and D. Walton, *Nature*, 1997, **388**, 52.

2 X. S. Li, W. Cai, J. An, S. Kim, J. Nah, D. Yang, R. Piner, A. Velamakanni, I. Jung, E. Tutuc, S. K. Banerjee, L. Colombo and R. S. Ruoff, *Science*, 2009, **324**, 1312.

3 S. C. Xu, B. Y. Man, S. Z. Jiang, C. S. Chen, C. Yang, M. Liu, X. G. Gao, Z. C. Sun and C. Zhang, *CrystEngComm*, 2013, **15(10)**, 1840.

4 A. Reina, X. Jia, J. Ho, D. Nezich, H. Son, V. Bulovic, M. S. Dresselhaus and J. Kong, *Nano Lett.*, 2009, **9(8)**, 3087.

5 C. Zhang, B. Y. Man, C. Yang, S. Z. Jiang, M. Liu, C. S. Chen, S. C. Xu, Z. C. Sun, X. G. Gao and X. J. Chen, *Nanotechnology*, 2013, **24**, 395603.

6 H. Chang and H. Wu, *Adv. Funct. Mater.*, 2013, **23(16)**, 1984.

7 S. Wang, Y. Zhang, N. Abidi and L. Cabrales, *Langmuir*, 2009, **25(18)**, 11078.

8 A. Siokou, F. Ravani, S. Karakalos, O. Frank, M. Kalbac and C. Galiotis, *Appl. Surf. Sci.*, 2011, **257(23)**, 9785.

9 J. Cheng and J. Du, *CrystEngComm*, 2012, **14(2)**, 397.

10 G. Jo, M. Choe, S. Lee, W. Park, Y. H. Kahng and T. Lee, *Nanotechnology*, 2012, **23(11)**, 112001.

11 Y. Zhang, L. Q. Ren, K. Zhang, S. R. Wang and J. J. Qiu, *Sci. Adv. Mater.*, 2013, **5(4)**, 366.

12 W. H. Yuan, B. Q. Li and L. Li, *Appl. Surf. Sci.*, 2011, **257(23)**, 10183.

13 W. Dang, H. Peng, H. Li, P. Wang and Z. F. Liu, *Nano Lett.*, 2010, **10(8)**, 2870.

14 H. M. Xu, G. Chen, R.C. Jin, J. Pei, Y. Wang and D. H. Chen, *CrystEngComm*, 2013, **15(8)**, 1618.

15 Y. Yan, Z. M. Liao, F. Yu, H. C. Wu, G. Y. Jing, Z. C. Yang, Q. Zhao and D. P. Yu, *Nanotechnology*, 2012, **23(30)**, 305704.

16 C. Han, J. Yang, C. Yan, Y. Li, F. Y. Liu, L. X. Jiang, J. C. Ye and Y. X. Liu, *CrystEngComm*, 2014, **16**, 2823.

17 C. L. Song, Y. L. Wang, Y. P. Jiang, Y. Zhang, C. Z. Chang, L. L. Wang, K. He, X. Chen, J. F. Jia, Y. Y. Wang, Z. Fang, X. Dai, X. C. Xie, X. L. Qi, S. C. Zhang, Q. K. Xue, and X. C. Ma, *Appl. Phys. Lett.*, 2010, **97(14)**, 143118.

18 W. Richter, H. Kohler, C. R. Becker, *Phys. Status Solidi B*, 1977, **84(2)**, 619.